

# Green synthesis of titanium dioxide nanoparticles with volatile oil of *Eugenia caryophyllata* for enhanced antimicrobial activities

Raghad Dhyea Abdul Jalil<sup>1</sup> ✉

<sup>1</sup>Department of Biology, College of Science, Mustansiriyah University, Baghdad, Iraq

✉ E-mail: stru@uomustansiriyah.edu.iq

ISSN 1751-8741

Received on 9th June 2017

Revised 19th December 2017

Accepted on 9th February 2018

E-First on 23rd April 2018

doi: 10.1049/iet-nbt.2017.0139

www.ietdl.org

**Abstract:** Different chemo-physical methods are used to synthesise titanium oxide nanoparticles (TiO<sub>2</sub> NPs), which are often expensive, unfriendly to the environment, toxic, not biocompatible, with a small yield. To resolve these problems, the researchers use green procedures to synthesise TiO<sub>2</sub>-NPs by plant extracts of *Capsicum annum* L. and *Allium cepa* (onion) and characterise using atomic force microscopy, scanning electron microscopy, transmission electronic microscopy, X-ray diffraction, ultraviolet (UV)–visible (Vis) spectra and Fourier transform infrared spectroscopy. The results indicate that most NPs synthesised by the first and second procedures of onion had an average diameter of 95.7 and 89.1 nm, while NPs synthesised by *C. annum* had an average diameter of 103.60 and 90.07 nm, respectively. In UV–Vis spectra, strong absorption was below 470 nm, and energy gap was 3.3 eV in each of the first procedure of *A. cepa* and the second procedure of *C. annum* compared with 270 nm, 6.3 eV for each of the second procedure of *A. cepa* and the first procedure of *C. annum*. The antimicrobial activities of NPs were evaluated and an attempt was made to enhance these activities by *Eugenia caryophyllata* plant's oil in combination therapies. There were synergistic effects between NPs and plant's oil.

## 1 Introduction

The Latin names of clove or Kabsh Qarunfil are *Syzygium aromaticum* (L.) (Merr. & Perry), *Eugenia caryophyllata* (Thunb.), and *Eugenia aromatica* (Kuntze.), and they belong to Myrtaceae family [1].

Traditionally, Qarunfil is used as a carminative and anti-inflammatory. Its aromatic bud flowers are used as anti-inflammatory, an antiseptic and peripheral anti-nociceptive activity [2], antiemetic, stimulant, treat dyspepsia, and gastric irritation. Oil employed as a local analgesic for hypersensitive dentine's and carious cavities; internally antispasmodic, topical anaesthesia [3]. Recently, an aqueous extract of *E. caryophyllata* (Qarunfil) was found to be the most efficient against *Salmonella typhi*, compared with *Klebsiella pneumonia* and *Escherichia coli* [4]. Essential oil (0.4%) was antibacterial (*Bacillus subtilis*, *E. coli*, *Staphylococcus aureus* and *Pseudomonas aeruginosa*), which are Gram-negative and -positive bacteria [5, 6], and anaerobic bacteria *Prevotella nigrescens* and *Porphyromonas gingivalis* [7], and anti-fungal activities against 53 clinical isolates of *Candida* [8]. The main chemical component in the buds' oil, which was analysed by gas chromatography–mass spectrometry, are eugenol (81.13–84.44%), eugenyl acetate (11.60–15.02%) and β-caryophyllene (3.45–4.60%), respectively, these compounds are present in leaves oil at 81.06–86.04%, 2.02–3.05% and 11.95–16.16%, and in stems oil eugenol is 97.20–98.83% [9, 10]. These activities of oil are due to eugenol. Eugenol and acetyleugenol exhibit cholagogue activity and could inhibit arachidonate-, adrenalin- and collagen-induced platelet aggregation. Qarunfil terpenes induced detoxifying enzyme, glutathione-S-transferase in mouse liver and intestine and could act as carcinogen detoxification. Whole qarunfils could exhibit chemoprotective activity against liver and bone marrow toxicity [3].

Nanoparticles (NPs; <100 nm) have unique properties compared with their bulk particles. TiO<sub>2</sub>-NPs are very important because they exhibit low cost, stability, high refractive index, high optical properties, high ultraviolet (UV) absorbance, low toxicity, and strong redox ability, TiO<sub>2</sub> has a high energy gap (i.e. 3.2–5.2 eV) [11], and has good electrical, optical and magnetic properties

[12, 13]. Different chemo-physical methods succeeded in synthesising TiO<sub>2</sub> NPs, which depends on the top down and down top method [14–16]. They are often high cost, unfriendly to the environment, toxic, biocompatible, with a small yield etc. [17].

To resolve these problems, the researchers tend to use biosynthesis, bio-nanotechnology or green synthesis, which usually refers to intersection between biotechnology and nanotechnology, including biomolecules produced by the plant, bacteria, virus, fungi etc.) to synthesise materials of nano-size, which are used in different nanotechnological applications [18]. In other words, it means, synthesis of nanomaterials by living organisms or biological systems [19, 20]. *Aloe vera* leaves extract was successfully used in synthesising TiO<sub>2</sub>-NPs with a tetragonal structure, their crystallite size was 12 nm as per X-ray diffraction (XRD) analysis and 30 nm (using a particle size analyser). The absorption spectrum of the anatase phase of TiO<sub>2</sub>-NPs is around 393 nm with 3.2 eV band gap [21]. In addition, spherical titanium dioxide NPs produced from nyctanthes leaves extract with a size range of 100 and 150 nm [22]. *Curcuma longa* is a good TiO<sub>2</sub>-NPs biosynthesising agent by two procedures. The average sizes were 76.36 and 92.6 nm, respectively, with good optical properties. The crystals had the following shapes: anatase, rutile, and brookite when the first procedure was used and was pure anatase when the second procedure was used [23].

TiO<sub>2</sub> NPs are used in different applications such as pigments, adsorbents, catalysts, supports, paints, sunscreens, toothpaste, ointments etc. [24, 25]. They also have biomedical applications such as anti-parasitic properties [26], anti-cancer treatment [27], reduce growth and sporulation of *Fusarium graminearum* and reduce damping-off due to these fungi in two varieties of wheat plants [23], with less effect on plant germinations [28]. TiO<sub>2</sub> NPs exhibit good antimicrobial activity, especially when exposed to visible light they absorb photocatalysts which successful kill *S. aureus* and *E. coli* [29], *P. aeruginosa*, *Enterococcus hire* and *Bacteroides fragilis*. This antimicrobial feature of TiO<sub>2</sub>-NPs could also be activated by UV light to kill bacteria in 60 min, so, it is easy to be used as antibacterial coatings in the mixture with paint in hospital [30, 31] and wastewater disinfection processes [32, 33]

but these NPs had either no toxicity in the dark [34] or a small anti-bacterial effect at 100 mg/ml when it is used alone, other studies found that it could be stimulated using combination therapies of mixing them (50 mg/ml) with 50 mg/ml of methanol extraction of *Citrullus colocynthis* which showed synergistic effects in each of *S. aureus* and *E. coli* [35].

The goals of the present study are to synthesise TiO<sub>2</sub> NPs via different green syntheses of *Allium cepa* and *Capsicum annum* plant extracts and characterised their crystallinity, crystallite size, band gap, functional group, and structural properties. The antimicrobial activities of green-synthesised NPs alone and volatile oil of *E. caryophyllata* alone and their combination therapy were, also, evaluated to understand their biological properties and if there are any synergistic effects between them.

## 2 Materials and methods

### 2.1 Green synthesis of TiO<sub>2</sub>-NPs using plant extraction

**2.1.1 Plant extraction:** Leaves of *A. cepa* (onions) and *C. annum* L were used for green synthesis. They were obtained from the Herbarium of Iraqi Ministry of Health who identified plants by a taxonomic method. Eighty grams of fresh parts of onion leaves were mixed with 250 ml of distal water by homogenised blender for 3 min. The extract was put on a hot plate with a magnetic stirrer at 50–60°C for 4–5 h, filtered by Whatman number four filter paper. The residue was removed. Ninety grams of fruit were mixed with 250 ml of distal water by using a homogenised blender for 3 min. The extract *C. annum* was put on a hot plate with a magnetic stirrer at 50–60°C for 4–5 h and filtered as described above. The filtrates were directly used for the green synthesis of NPs.

**2.1.2 Synthesis:** *A. cepa*: 50 ml of plant extract were mixed with 1 ml of (50 mg/ml) of bulk TiO<sub>2</sub> particles (Sigma-Aldrich, China; anatase crystal form, their size was >2 μm) in a flask, placed in a magnetic stirrer hot plate at 50°C with 1000 rpm for 4–5 h, this was the first procedure while in the second procedure, a magnetic stirrer plate at 25 ± 3°C with 1000 rpm for 48 h.

*C. annum*: for the first procedure, 50 ml of plant extract were mixed with 1 mm of (50 mg/ml) of bulk TiO<sub>2</sub> particles in the flask, placed in a magnetic stirrer hot plate at 50°C with 1000 rpm for 4–5 h. In the second procedure, 50 ml of plant extract were mixed with 200 μl of (100 mg/ml) of bulk TiO<sub>2</sub> particles in the flask, placed in a magnetic stirrer plate at 25 ± 3°C with 1000 rpm for 48 h.

The supernatant was neglected. The precipitate was washed with double distilled water, centrifuged at 1500 rpm for 10 min. This was repeated three times. The obtained precipitate was dried at 25 ± 2°C for 24 h. It is characterised as follows [23].

**Characterisation:** The following techniques were used for the characterisation of NPs: atomic force microscopy (AFM), (Shimadzu-Japan, AA3000), at the Center of Nanotechnology and Advanced Materials, the University of Technology, Iraq [36]. A UV-visible spectrum (Schimadzu 1601 spectrophotometer) in the 200–800 nm range [37]. Transmittance measurements, coefficients of absorption and gap energy were calculated for the optical properties and described according to [38]. XRD (Shemadzu, Japan) was used to confirm crystal phases and sizes of each phase. XRD analysis was performed using an X-ray diffractometer with Cu-Kα crystal radiation (λ = 1.54056 Å) scanning at a rate of 5°/min for (2θ) range of 20°–70°. The samples' diffraction peaks were identified by comparison (00-021-1272 card, variable slit intensity). The full width at half maximum (FWHM) and Scherer's equation were used to determine the crystallite size [39]. The strain value η [40] and the dislocation densities δ values [41] were also calculated. Scanning electron microscope (SEM) (Vega Tescan, USA), at the University of Technology, the Centre for Nanotechnology and Advanced Materials, Iraq, was utilised to analyse NPs. To determine the size and morphology of NPs, transmission electronic microscopy (TEM) analysis (Philips CM10 electron microscope operating at 60 kV) was used according to the procedure of College of Medicine, Al Nahrin University. Fourier transform infrared spectroscopy (FT-IR, Shemadzu, Germany) was

utilised to determine the various functional groups present in TiO<sub>2</sub> in the Central Service Laboratory, University of Baghdad, College of Education and Pure Sciences, Ibn Al-Haitham, Iraq.

### 2.2 Antimicrobial activities

**2.2.1 Preparation:** Volatile oil of *E. caryophyllata* was brought from Al-Emad factory, Iraq. Tween 5% was used to dilute it. Sterilised distilled water used to prepare several concentrations of bulk particles of TiO<sub>2</sub>, standard NPs, green synthesis of nanoparticles, which were synthesised by the second procedure of *A. cepa* and *C. annum* plant extracts.

**2.2.2 Experiments:** The antimicrobial activities were estimated against four species of bacteria: *S. aureus*, *K. pneumonia*, *Staphylococcus epidermidis*, and *E. coli* and one isolate of *Candida albicans*, which were obtained from the Department of Biology, College of Science, AL-Mustainsiriyah University, Baghdad, Iraq.

The dilution broth susceptibility procedure was used for the antimicrobial activity [42]. Six treatments were found, each treatment deals with various concentrations. These were TiO<sub>2</sub> bulk particles, TiO<sub>2</sub> NPs produced by the second procedure of *A. cepa* alone, TiO<sub>2</sub> NPs produced by the second procedure of *C. annum* alone, volatile oil of *E. caryophyllata* alone, a combination therapy of NPs synthesised by the second procedure of *A. cepa* with volatile oil and finally combination therapy of NPs synthesised by the second procedure of *C. annum* with volatile oil.

One drop of each tested culture strain was added to 10 ml of nutrient broth, these were serially diluted five times. One drop (from dilute 5) was added to solution A (which was made up of 1 ml of nutrient broth and 1 ml sample), incubated at 37°C for 24 h, then diluted seven times. The seventh dilution was seeded by streaking the surface of nutrient agar medium and incubated at 37°C for 24 h. A negative control and three replicates of each treatment were found. The percentage of reduction was calculated by using the following equation:

$$IR\% = (A - B)/A \times 100, \quad (1)$$

where *R* is the percentage of reduction of the number of colonies, *A* is the colony number of bacteria in control treatment and *B* is the number of colonies of bacteria after the transaction article NPs.

The determination of the synergistic effects of TiO<sub>2</sub>-NPs and volatile oil of *E. caryophyllata* combination treatment was carried out according to [43]. The Compusyn Computer Software (version 2011) was used for determining the combination index (CI) from drug cytotoxicity and a combination of synergistic, additive, or antagonistic was determined.

## 3 Results and discussion

### 3.1 Green synthesis

AFM: the calculated TiO<sub>2</sub> NPs' sizes were calculated using the software of the AFM. For the first and second procedures of *A. cepa*, size particles ranged 20–170 and 20–160 nm with an average diameter of 95.7 and 89.1 nm (Fig. 1a), while the size of NPs produced by the first and second procedures of the *C. annum* plant extract was 103.60 and 90.07 nm, respectively (Fig. 1b). Figs. 2a–d show AFM topographic images of green synthesised TiO<sub>2</sub>-NPs. Roughness averages (Ra) were 3.18 and 1.98 nm, root mean squares (Sq) were 3.72 and 2.3 nm for the first and second procedures of *C. annum* plant extract. SEM analysis found the formation of agglomerates containing spherical nano-size particles with an approximate diameter of ~100 nm for the first and second procedures of *A. cepa* (Figs. 3a and b) compared with 90 nm for the second procedure of *C. annum* plant extract (Figs. 3c and d). Figs. 4a and b show TEM images of green synthesised NPs by the first procedure of *A. cepa* with an average particle size of 68.7 nm compared with particle size around 20 and 40 nm by the second procedure of *A. cepa*. Figs. 4c and d show TEM images of TiO<sub>2</sub> produced by the first procedure (size: 15 and 46 nm) and second

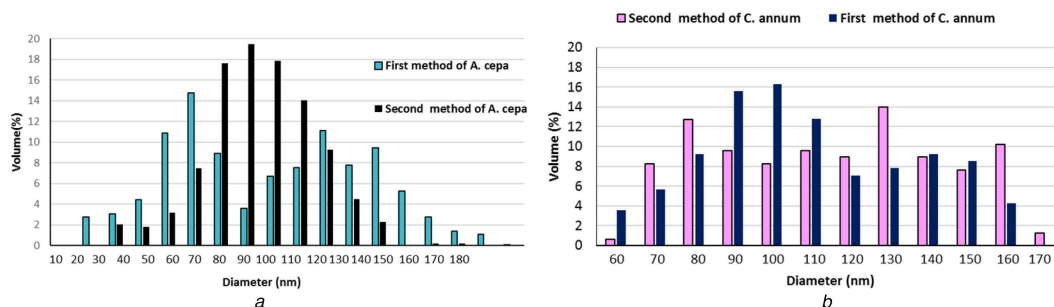


**Fig. 1** Granularity volume distribution chart of TiO<sub>2</sub>-NPs synthesised by the first and second procedures of (a) *A. cepa*, (b) *C. annuum*

procedure (size: 38 and 108 nm) of *C. annuum* plant extracts. All particles were spherical

The data of XRD of all samples indicated that the structures were rutile and anatase. The XRD pattern of the first and second procedures of *A. cepa* NPs showed six and five peaks, respectively. Strong diffraction peaks were 25.305° (101), 48.052° (200), 55.09° (323), 37.8° (004), 53.88° (105), which were anatase crystals and 36.2° (101), rutile crystals, for the first procedure of *A. cepa* (Fig. 5a) and 25.217° (101), 47.946° (200), 37.684° (004), 37.8° (004), 53.3° (105), for the second procedure of *A. cepa* which were anatase and 36.04° (101), rutile crystals (Fig. 5b).

Strong peaks produced by the first procedure of *C. annuum* were 25.1103° (101), 37.5897° (004), 54.9° (105), 62.48° (204) which were anatase crystals and 27.6° (101), 27.88° (101) for rutile crystals (Fig. 5c). Strong peaks produced by the second procedure of *C. annuum* were 25.324° (101), 48.054° (200), 37.832° (004), and 55.08° (307), their crystal shapes were anatase (Fig. 5d). The average crystallite sizes were 39.16, 44.54 and 43.164, and 54.867 nm, respectively (Table 1).

The data of UV-Vis spectra found that the absorption spectra and optical band gaps of TiO<sub>2</sub>-NPs produced by the first procedure of *A. cepa* were exactly the same in NPs produced by the second procedure of *C. annuum*, strong absorption below 470 nm, and energy gap was 3.3 eV (Fig. 6a). There was another similarity found between the second procedure of *A. cepa* and the first procedure of *C. annuum*, their strong absorption and energy gaps were 270 nm and 6.3 eV respectively (Fig. 6b).

In FT-IR spectra, samples exhibited absorption peaks at 528, 685, and 536, 685 cm<sup>-1</sup> for the first and second procedures of *A. cepa*, respectively, which indicates the presence a Ti-O stretching bond. The 1637 and 1639 cm<sup>-1</sup> for the first and second procedures of *A. cepa*, respectively, indicated the presence of an O-Ti-O stretching bond, in addition to 1458 and 1541 cm<sup>-1</sup> (the second procedure of *A. cepa*) which indicates the presence Ti-O-Ti (Figs. 7a and b).

In the first procedure of *C. annuum*, the strong peak located at 509 and 671 cm<sup>-1</sup> in addition to 1442 cm<sup>-1</sup> indicated the presence of Ti-O stretching while the peak at 1036 cm<sup>-1</sup> corresponds to Ti-O/Ti-O-C and 1647 cm<sup>-1</sup> indicating O-Ti-O (Fig. 7c). In the second procedure of *C. annuum*, the strong peak located at 528 and 679 cm<sup>-1</sup> corresponds to the Ti-O stretching bond. The peaks at 1043, 1076 and 1151 cm<sup>-1</sup> indicated Ti-O/Ti-O-C; moreover, the peak at 1647 cm<sup>-1</sup> corresponds to the O-Ti-O stretching bond (Fig. 7d).

The current study succeeded in synthesising TiO<sub>2</sub>-NPs by *A. cepa* and *C. annuum* plant extracts. The authors of [44] showed that these NPs had a high energy gap and high absorption coefficient than the traditional physiochemical procedure, they were around 351–362 nm and about 3.54–3.43 eV, which was prepared via two different routes: (i) the sol-gel route and (ii) the hydrothermal procedure, respectively [44], and compared with TiO<sub>2</sub> fabricated by the hydrazine procedure with an energy gap of 3.36 eV for sample N, 3.32 eV for sample H, and 3.2 eV for sample C [45]. The band gap changes in the present results mainly due to the presence of stress applied along the weak direction of the anatase crystal [46].

TiO<sub>2</sub>-NPs were fabricated by different plant extracts, *A. vera* leaves' extract is an example of a synthesised tetragonal structure with crystallite size of 12 nm in XRD analysis. The absorption spectrum of the TiO<sub>2</sub> sample was 393 nm with a band gap of the anatase phase (~3.2 eV) [21]. Moreover, *C. longa* succeeds in biosynthesising TiO<sub>2</sub>-NPs by two procedures with average sizes of 76.36 and 92.6 nm, respectively, and crystal shapes were of three forms: brookite, rutile, and anatase when the first procedure was used and it was pure anatase when the second procedure was used, their average sizes were 22.881 and 43.088 nm for colloidal solution and nano-powder, respectively, in the first procedure and 45.808 nm for nano-powder in the second procedure while in the current study, the average crystallite sizes were 39.16, 44.54 and 43.22 nm for the first and second procedures of *A. cepa* and *C. annuum*, respectively [23]. Similar observations were made on spherical TiO<sub>2</sub>-NPs produced from nycatanthes leaves extract, particles' sizes in the range of 100–150 nm [22] and by *Ailanthus altissima* plant extract [47].

Onion (family: Amaryllidaceae) contains phenolic substances especially quercetin, phenolic acids, sulphur, compounds (allicin), alkaloids, flavonoids, terpenes, steroids, vitamins and minerals [48], fructose, quercetin-3-glucoside, isorhamnetin-4-glucoside, mannose, galactose, glucose, xylose, organosulphur, compounds, thiosulphates, S-alk(en)yl cysteine sulphoxides, flavonoids, flavonols, selenium, cycloalliin, allylsulphides, seleno compounds and sulphur [49–51]. It can reduce gold to NPs due to vitamin C in onion extract [52]. Abdul Jalil and others in 2017 [53] had reported using *A. cepa* and *C. annuum* plant extracts, acting as the reducing agent for fabricating ZnO NPs of well-defined dimensions [53].

### 3.2 Antimicrobial activities

**3.2.1 NPs and bulk particles alone:** In this experiment, three treatments were found: TiO<sub>2</sub>-NPs synthesised by *A. cepa*, TiO<sub>2</sub>-NPs synthesised by *C. annuum* and bulk particles of TiO<sub>2</sub>, each of them was used alone. *K. pneumonia* was not affected by all concentrations of bulk particles alone while bacteria were either not affected or stimulated by NPs alone (Figs. 8a and b), while there were good activities against *S. epidermidis*, *S. aureus*, *E. coli* and *C. albicans* with significant differences ( $P \leq 0.05$ ) between the means of NPs compared with control except for *S. epidermidis* which had low reduction by the NPs synthesised by *C. annuum*. All concentrations of NPs synthesised by *A. cepa* were more reducer to *S. aureus* compared with each of the bulk particles and NPs synthesised by *C. annuum*, while in *E. coli* these effects were seen at lower concentrations (0.01–1 mg/ml) and the opposite was, also, seen at higher concentrations (Fig. 8c). NPs synthesised by *A. cepa* were more reducer to all tested organisms than bulk particles and it was more reducer than NPs synthesised by *C. annuum*. This might be due to the presence of the rutile crystal in NPs synthesised by *C. annuum* and absence of NPs synthesised by *A. cepa* as seen in XRD analysis.

**3.2.2 Volatile oil of *E. caryophyllata* alone:** There were good activities of all dilutions of oil alone against *C. albicans* and *S. epidermidis* with significant differences ( $P \leq 0.05$ ) between the

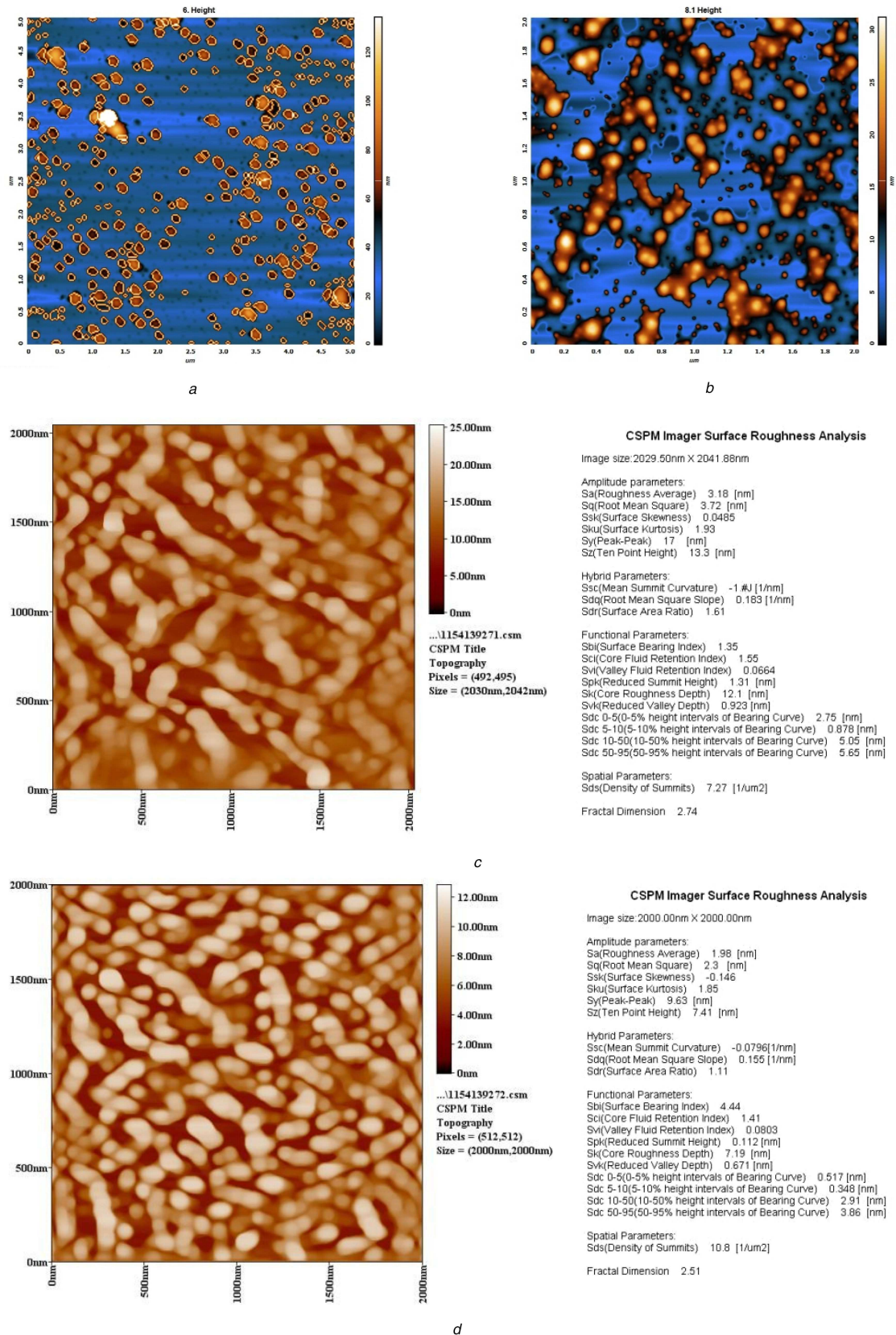


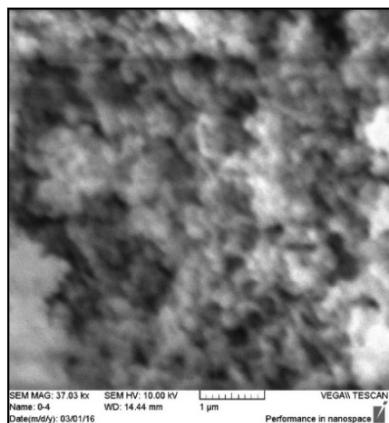
**Fig. 2** AFM topographic images of  $TiO_2$  NPs synthesis by (a) First procedure of *A. cepa*, (b) Second procedure of *A. cepa*, (c) First procedure of *C. annuum*, (d) Second procedure of *C. annuum*

means of NPs compared with control. The inhibition rate ranges from 79.74 to 93.16 and 79.07 to 86.3, respectively. *K. pneumonia* was less effective with IR% ranging from 31.82 to 45.45. *S. aureus* was reduced by most concentrations of oil except 12.5%, which induced growth (Fig. 9).

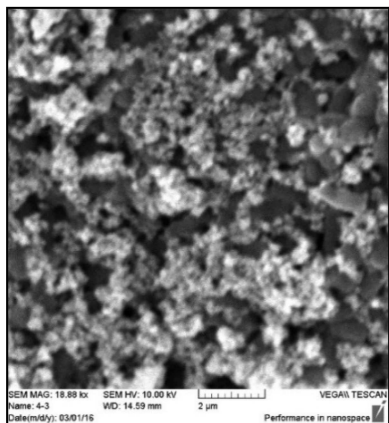
All dilutions of oil alone were more reducer to *K. pneumonia*, *S. epidermidis* and *C. albicans* than NPs alone, while other bacteria

were more reducer in dose-dependent manner. The toxicity of this plant alone is probably because of some components which were found in oils, especially eugenol 81.13 to 84.44% and eugenyl acetate (11.60–15.02%) or  $\beta$ -caryophyllene (3.45–4.60%) [10].

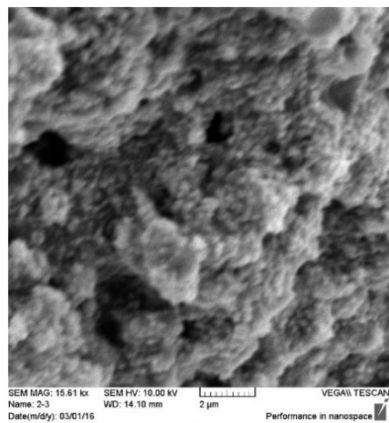
**3.2.3 Combination therapy:** In combination therapy, different dilutions of volatile oils of *E. caryophyllata* were performed with



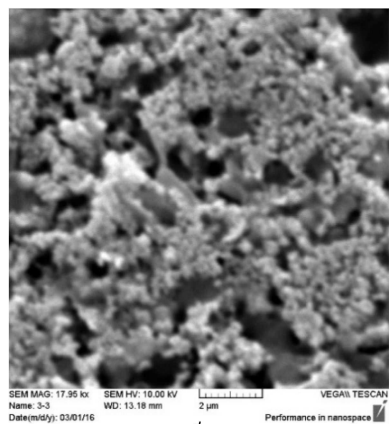
a



b

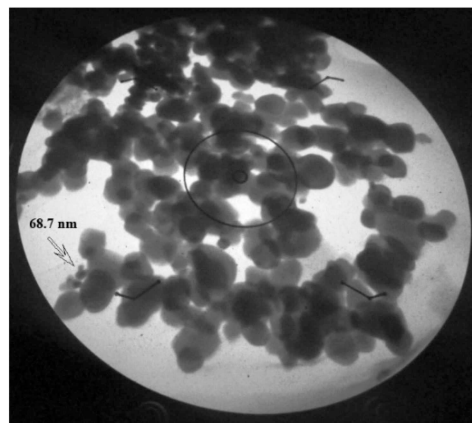


c

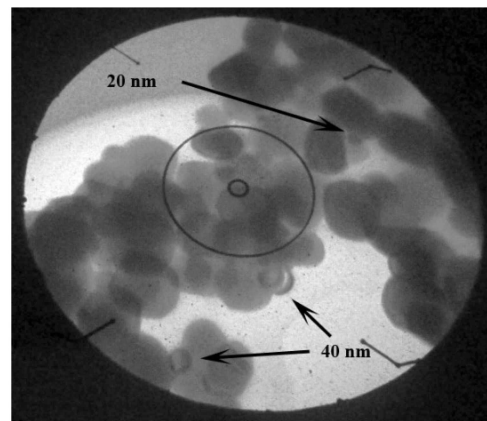


d

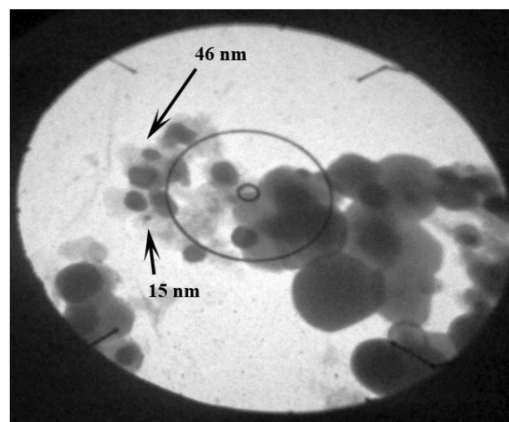
**Fig. 3** SEM images of  $\text{TiO}_2$ -NPs synthesised by (a) First procedure of *A. cepa* (<100 nm), (b) Second procedure of *A. cepa* (<100 nm), (c) First procedure of *C. annuum* (<95 nm), (d) Second procedure of *C. annuum* (<90 nm)



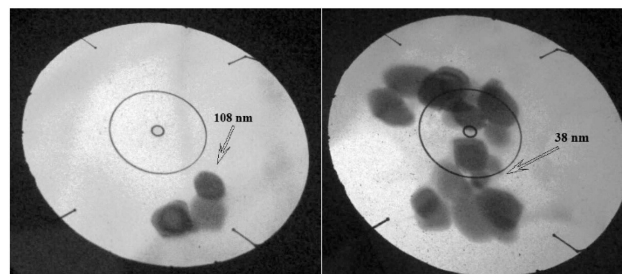
a



b



c



d

**Fig. 4** TEM of  $\text{TiO}_2$  produced by using (a) First procedure of *A. cepa* plant extracts (68.7 nm) at 92,000 $\times$  magnification, (b) Second procedure of *A. cepa* plant extracts (20, 40 nm) at 130,000 $\times$  magnification, (c) First procedure of *C. annuum* plant extracts (15, 46 nm), (d) Second procedure of *C. annuum* plant extracts (38, 108 nm) at 130,000 $\times$  magnification

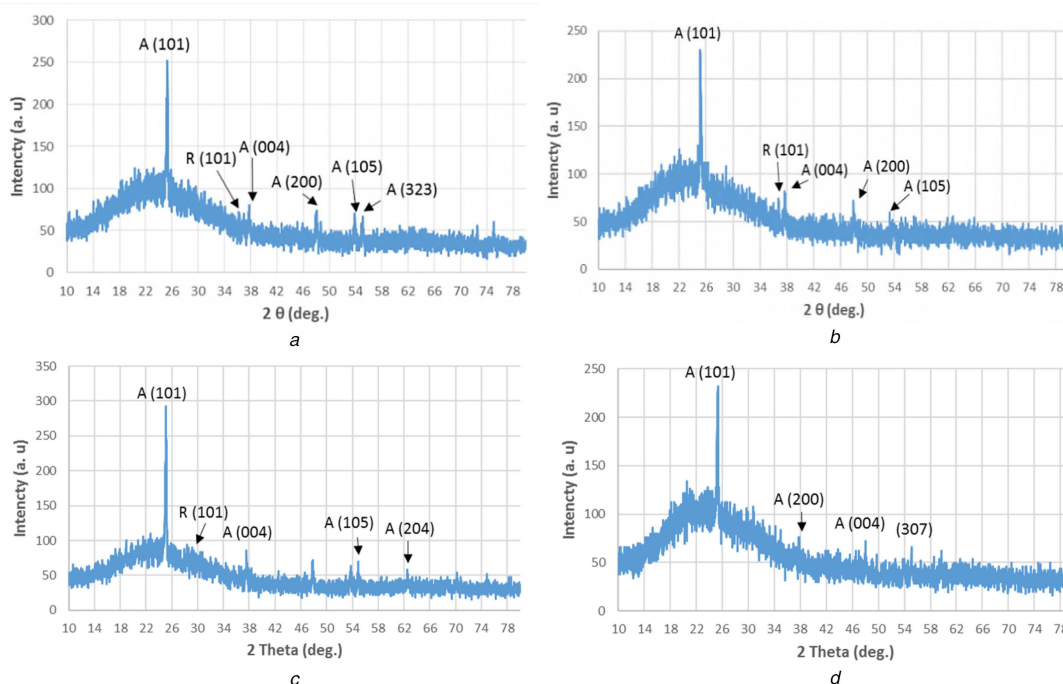


**Fig. 5** X-ray pattern of  $\text{TiO}_2$ -NPs synthesised by (a) First procedure of *A. cepa*, (b) Second procedure of *A. cepa*, (c) First procedure of *C. annuum*, (d) Second procedure of *C. annuum*

**Table 1** Summary of X-ray characterisation of green synthesised  $\text{TiO}_2$  NPs by the first and second procedures of *A. cepa* and *C. annuum* plant extracts

Sample	Planes ( $hkl$ )	$2\theta$ , °	FWHM, °	$D$ , nm	Strain XE-4	DIS X1014
first procedure of <i>A. cepa</i>	101	25.305	0.225	36.027	38.471	7.704
	200	48.052	0.193	44.791	30.944	4.985
	323	55.094	0.243	36.671	37.796	7.436
second procedure of <i>A. cepa</i>	101	25.217	0.199	40.630	34.113	6.058
	200	47.946	0.167	51.916	26.697	3.710
	004	37.684	0.203	41.084	33.736	5.925
first procedure of <i>C. annuum</i>	101	25.110	0.219	36.967	37.493	7.318
	200	47.838	0.197	43.979	31.515	5.17
	004	37.589	0.172	48.547	28.55	4.243
second procedure of <i>C. annuum</i>	101	25.324	0.195	41.598	33.319	5.779
	200	48.054	0.15	57.721	24.012	3.002
	004	37.832	0.128	65.282	21.231	2.347

( $hkl$ ) planes: crystallographic plane; FWHM: full width at half maximum;  $D$ : dimension of crystal in nm;  $\eta \times 10^{-4}$ : strain value;  $\delta \times 10^{14}$ : dislocation density.

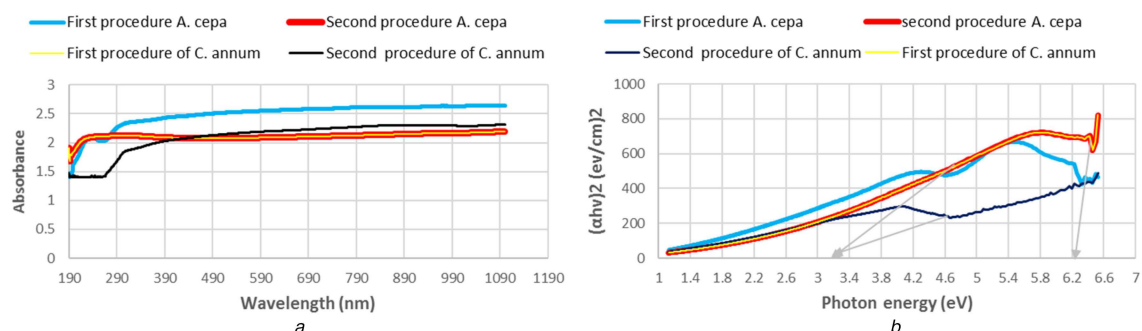


**Fig. 6** UV-vis study of green synthesis  $\text{TiO}_2$  NPs using the first and second procedures of *A. cepa* and the first and second procedures of *C. annuum* plants extracts.

(a) absorptions spectrum, (b)  $(ah\nu)^2$  versus photon energy and estimated optical absorption bandgap.

various concentrations of NPs synthesised by *A. cepa* and *C. annuum*. Results proved statistically significant difference ( $P \leq 0.05$ ) between all concentrations of combination therapies of NPs synthesised by *A. cepa* with oil plants on all different organisms under study compared with control (Fig. 10a). The same results

were obtained using combination therapy of NPs synthesised by *C. annuum* with volatile oil (Fig. 10b).

**3.2.4 Synergistic effect:** In combination therapy between NPs synthesised by *A. cepa* and volatile oil, the results found four synergistic combination points in *S. aureus*, one synergistic

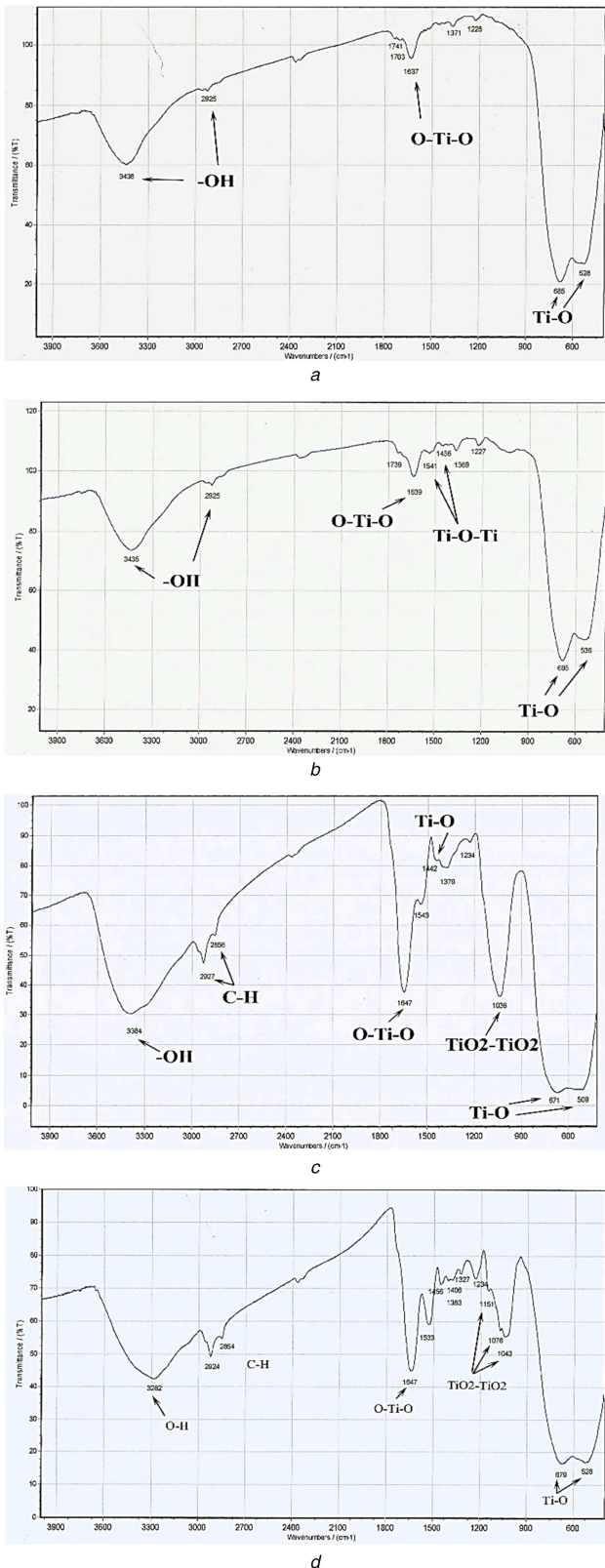


**Fig. 7** FT-IR spectra of TiO<sub>2</sub> produced by using (a) First procedure of *A. cepa* plant extracts, (b) Second procedure of *A. cepa* plant extracts, (c) First procedure of *C. annuum* plant extracts, (d) Second procedure of *C. annuum* plant extracts

combination point in *E. coli* and three synergistic combination points in *C. albicans*, the combination was tested at the 50% inhibitory concentration level. All combination points were located in the antagonism area in *K. pneumonia* and *S. epidermidis* (Table 2). While from the CI of combination therapy between NPs synthesised by *C. annuum* with volatile oil there was one synergistic combination point in each of *K. pneumonia*, *S. epidermidis*, and *S.*

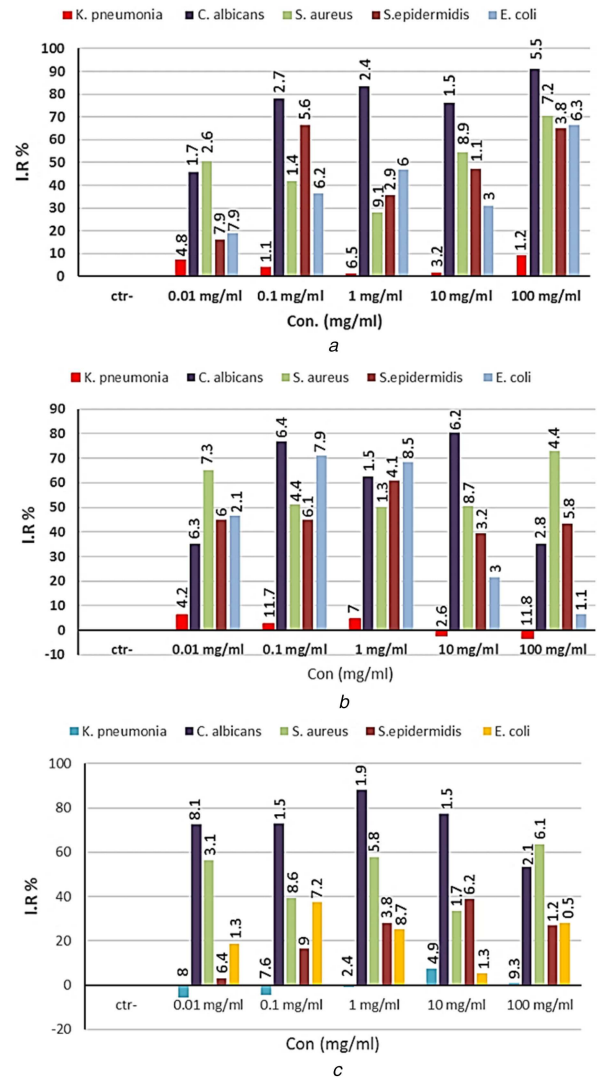


**Fig. 8** Antibacterial activity of (a) Bulk TiO<sub>2</sub> particles alone, (b) TiO<sub>2</sub> NPs alone synthesised by *A. cepa*, (c) TiO<sub>2</sub> NPs alone synthesised by the second procedure of *C. annuum*. IR%: inhibition rate, Con.: concentration. The numbers above the bars are standard errors

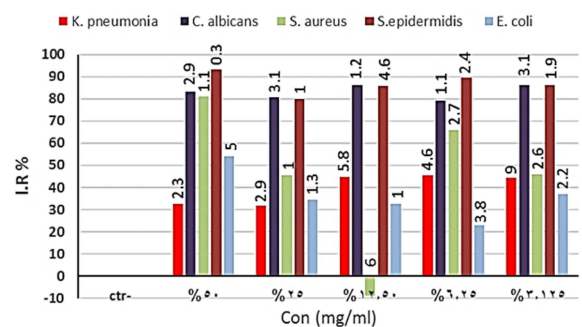


**Fig. 9** Antibacterial activity of *E. caryophyllata* oil alone. IR%: inhibition rate, Con.: concentrations. The numbers above the bars are standards errors

*aureus* while there were four synergistic combination points in each of *C. albicans* and *E. coli* (Table 3).

Combination therapy is the standard of care since it is a rational strategy to raise responses and tolerability's and to reduce resistance. Many different combination therapies are under investigation to facilitate some synergistic interactions between therapies which may permit lower concentration of agents to be used to minimise both cost and toxicity.

Some studies found that these NPs had either no toxicity in the dark [34] or a small anti-bacterial effect at 100 mg/ml when they

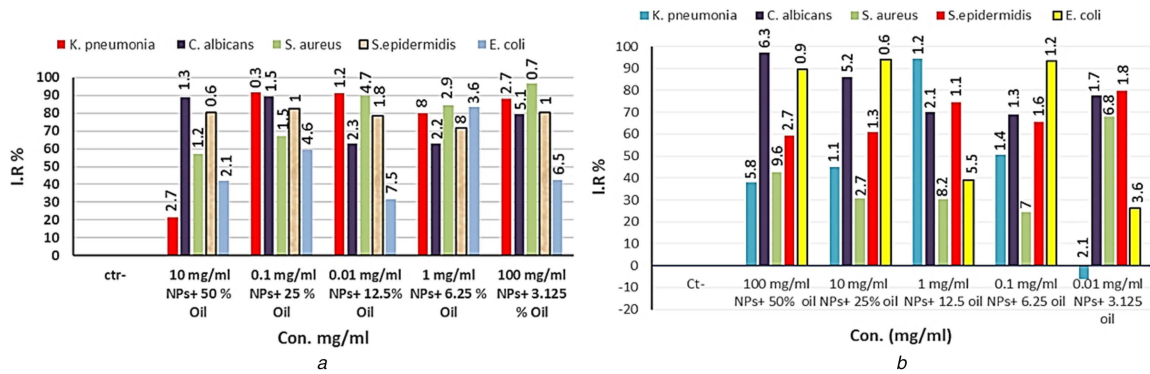


**Fig. 10** Antibacterial activity of combination therapy between oil of *E. caryophyllata* and each NP synthesised by the second procedure of (a) *A. cepa*, (b) *C. annum*. IR%: inhibition rate, Con.: concentrations. The numbers above the bars are standards errors

**Table 2** CI data for non-constant combination (oil plants with NPs synthesised by the second procedure of *A. cepa*) on different bacteria species

Point	Dose		I.C.				
	NPs, mg/ml	Plant oil, %	<i>K. pneumonia</i>	<i>S. aureus</i>	<i>S. epidermidis</i>	<i>E. coli</i>	<i>C. albicans</i>
1	10	50	98.4767	85.3019	$7.02 \times 10^{43}$	1.54155	40,051.8
2	0.1	25	436,871	$2.45 \times 10^{-4}$	$1.96 \times 10^{45}$	115.284	38,626.1
3	0.01	12.5	166,536	$1.89 \times 10^{-6}$	$4.42 \times 10^{37}$	1.84991	$2.11 \times 10^{-9}$
4	1	6.25	1409.76	$3.61 \times 10^{-6}$	$2.17 \times 10^{29}$	$1.50 \times 10^{22}$	$1.32 \times 10^{-7}$
5	100	3.125	17,006	$1.49 \times 10^{-8}$	$3.98 \times 10^{44}$	<b>0.08953</b>	<b>0.0013</b>

Bold I.C. (<1): synergistic effect, I.C. (>1): antagonism effect, I.C. (=1): additive.

**Table 3** CI data for non-constant combination (oil plant with NPs synthesised by the second procedure of *C. annum*) on different bacteria species

Point	Dose		I.C.				
	NPs, mg/ml	Plant oil, %	<i>K. pneumonia</i>	<i>S. aureus</i>	<i>S. epidermidis</i>	<i>E. coli</i>	<i>C. albicans</i>
1	100	50	11,938.4	$3.69 \times 10^{13}$	$4.54 \times 10^{16}$	$1.08 \times 10^{10}$	0.02445
2	10	25	684.146	7819.84	$3.47 \times 10^{16}$	<b>0.05994</b>	$6.00 \times 10^{-13}$
3	1	12.5	525.967	339.669	144,690	<b>0.02587</b>	$6.29 \times 10^{-4}$
4	0.1	6.25	39.3592	<b>0.00227</b>	<b>0.26187</b>	<b>0.00543</b>	$3.26 \times 10^{-4}$
5	0.01	3.125	$6.51 \times 10^{-4}$	$4.70 \times 10^{31}$	5,302,729	$7.90 \times 10^{-4}$	$1.20 \times 10^{-10}$

Bold I.C. (<1): synergistic effect, I.C. (>1): antagonism effect, I.C. (=1): additive.

were used alone, but they could stimulate their antimicrobial activities especially under visible light absorbing photocatalysts which successfully kill *E. coli* and *S. aureus* [29], *P. aeruginosa*, *E. hire*, *E. coli*, *B. fragilis* and *S. aureus* or by UV light to kill bacteria in 60 min, so, it is easy to have antibacterial coatings mixed with paint in hospital. Recently, Abdul Jalill and Alli [35] found that it could be stimulated by the combination therapies of mixing them (50 mg/ml) with 50 mg/ml of methanol extraction of *C. colocynthis* which showed synergistic effects on *E. coli* and *S. aureus* [35].

In the current study, combinations of TiO<sub>2</sub>-NPs with *E. caryophyllata* oil showed four synergistic combination points in *S. aureus*, one synergistic combination point in *E. coli* and three synergistic combination points in *C. albicans*. This is the first time that TiO<sub>2</sub>-NPs with *E. caryophyllata* oil have been used as an antibacterial combination therapy.

Combination therapy is a common treatment for antimicrobial treatments, such as bee venom, its components, melittin and many plant' secondary metabolites like benzyl isothiocyanate, sanguinarine, carvacrol, and berberine, which are mixed with antibiotics mostly more efficient than each of the treatment alone [54, 55].

The data of [56] suggest that the plants (*Embllica officinalis* and *Nymphae odorata*), which may be used with the antibiotic, amoxicillin, against methicillin resistant *S. aureus* infection alone or with combination [56]. Moreover, there was the highest and strong synergism between *Carica papaya* methanolic extract in

combination with some antibiotics against bacterial strains [57]. Moreover, essential oils in addition to their combination with antibiotics/plant extracts have novel antimicrobial agents against multidrug resistant pathogenic microorganisms [58]. In addition, *S. aureus* killed by was potentiate when enterocin AS-48 was used in combination therapies with the phenolic compounds carvacrol, geraniol, eugenol, terpineol, caffeic acid, *p*-coumaric acid, citral, and hydro-cinnamic acid and these treatments were more efficient than each of them alone [59]. Recently, there was the synergistic activity of ZnO-NPs with some antibiotics to resist: fungi, negative and positive gram bacteria [60].

#### 4 Conclusions and recommendations

TiO<sub>2</sub>-NPs could be produced by plant extracts of *A. cepa* and *C. annum*, most of these particles (but not all) were smaller than 100 nm, they had antimicrobial properties against some species of microbes when they were used alone. There were different antimicrobial activities of bulk particles and NPs alone in dose-dependent manner against *E. coli*, *S. aureus*, *C. albicans*, and *S. epidermidis*. In addition, *K. pneumonia* was not affected by all concentrations of bulk particles alone while bacteria were either not affected or stimulated by NPs alone. Most dilutions of volatile oil of *E. caryophyllata* alone had antimicrobial activities.

Combination therapies reduced all studied organisms with different inhibition rates. There were four synergistic combination points of NPs synthesised by *A. cepa* with oil in *S. aureus*, one synergistic combination point in *E. coli* and three synergistic points



in *C. albicans*. All points located in the antagonism area in *K. pneumonia* and *S. epidermidis*. While in the combination therapy of NPs synthesised by *C. annuum* with oil, there was one synergistic point in each of *K. pneumonia*, *S. aureus* and *S. epidermidis* and four synergistic points in each of *C. albicans* and *E. coli*. In addition, all points in *S. aureus* are located in the antagonism area. Optimised other conditions for synthesising NPs such as charge, pH, pressure, and light, the exposure time will be helpful and more studies on detection of mechanical effects will be more beneficial.

## 5 Acknowledgments

The authors would like to thank Al-Mustansiriyah University (www.uomustansiriya.edu.iq) Baghdad, Iraq for its support of the current work.

## 6 References

[1] Milind, P., Deepa, K.: 'Clove: a champion spice', *Int. J. Res. Ayurveda Pharmacy*, 2011, **2**, (1), pp. 47–54

[2] Daniel, A.N., Sartoretto, S.M., Schmidt, G., et al.: 'Anti-inflammatory and antinociceptive activities of eugenol essential oil in experimental animal models', *Braz. J. Pharmacognosy*, 2009, **19**, (1B), pp. 212–217

[3] Khare, C.P.: 'Indian medicinal plants: an illustrated dictionary' (Springer-Verlag Berlin/Heidelberg 2007), p. 836

[4] Joshi, B., Sah, G.P., Basnet, B.B., et al.: 'Phytochemical extraction and antimicrobial properties of different medicinal plants: *Ocimum sanctum* (Tulsi), *Eugenia caryophyllata* (Clove), *Achyranthes bidentata* (Datiwan) and *Azadirachta indica* (Neem)', *J. Microbiol. Antimicrobials*, 2011, **3**, (1), pp. 1–7

[5] Fagere, Z.O., Al Magbou, A.Z.: 'Antibacterial activity of clove oil against some microorganisms at Khartoum state, Sudan', *Adv. Med. Plant Res.*, 2016, **4**, (4), pp. 122–128

[6] Nuñez, L., Aquino, M.D.: 'Microbicide activity of clove essential oil (*Eugenia caryophyllata*)', *Braz. J. Microbiol.*, 2012, **43**, (4), pp. 1255–1260

[7] Sousa, R.M.F., Morais, S.A.L., Vieira, R.B.K., et al.: 'Chemical composition, cytotoxic, and antibacterial activity of the essential oil from *Eugenia calycina* cambess leaves against oral bacteria', *Ind. Crops Prod.*, 2015, **65**, pp. 71–78

[8] Chaieb, K., Zmantar, T., Ksouri, R., et al.: 'Antioxidant properties of the essential oil of *Eugenia caryophyllata* and its antifungal activity against a large number of clinical *Candida* species', *Mycoses*, 2007, **50**, pp. 403–406

[9] Kennouche, A., Benkaci-Ali, F., Scholl, G., et al.: 'Chemical composition and antimicrobial activity of the essential oil of *Eugenia caryophyllata* cloves extracted by conventional and microwave techniques', *J. Biol. Act. Prod. Nat.*, 2015, **5**, (1), pp. 1–11

[10] Sohilaith, H.J.: 'Chemical composition of the essential oils in *Eugenia caryophyllata*, (Thunb.) from Amboina Island', *Sci. J. Chem.*, 2015, **3**, (6), pp. 95–99

[11] Bhakat, C.: 'Uniform TiO<sub>2</sub> nanoparticles synthesis and characterization by hemolysis process', *Int. J. Eng. Sci. Technol.*, 2012, **4**, (07), pp. 3081–3085

[12] Ramakrishna, G., Ghosh, H.N.: 'Optical and photochemical properties of sodium dodecylbenzenesulfonate (DBS)-capped TiO<sub>2</sub> nanoparticles dispersed in nonaqueous solvent', *Langmuir*, 2003, **19**, (3), pp. 505–508

[13] Sahni, S., Reddy, S.B., Murty, B.S.: 'Influence of process parameters on the synthesis of nano-titania by sol-gel route', *Mater. Sci. Eng.*, 2007, **A**, **452–453**, pp. 758–762

[14] Nguyen, T.V., Nguyen, T.A., Dao, P.H., et al.: 'Effect of rutile titania dioxide nanoparticles on the mechanical property, thermal stability, weathering resistance and antibacterial property of styrene acrylic polyurethane coating', *Adv. Nat. Sci., Nanosci. Nanotechnol.*, 2016, **7**, (4), pp. 1–9

[15] Lucky, R.A.: 'Synthesis of TiO<sub>2</sub>-based nanostructured materials using a sol-gel process in supercritical CO<sub>2</sub>'. Thesis for the Degree of Doctor of Philosophy, School of Graduate and Postdoctoral Studies, The University of Western Ontario, London, Ontario, Canada, 2008

[16] Ahmed, M.A., El-Shennawy, M., Althomali, Y.M., et al.: 'Effect of titanium dioxide nano particles incorporation on mechanical and physical properties on two different types of acrylic resin denture base', *World J. Nano Sci. Eng.*, 2016, **6**, pp. 111–119

[17] Narayanan, K.B., Sakthivel, N.: 'Biological synthesis of metal nanoparticles by microbes', *Adv. Colloid Interface Sci.*, 2010, **156**, pp. 1–13

[18] Douglas, T., Strable, E., Willits, D., et al.: 'Protein engineering of a viral cage for constrained nanomaterials synthesis', *Adv. Mater.*, 2002, **14**, (6), pp. 415–418

[19] Makarov, V.V., Love, A.J., Sinitsyna, O.V., et al.: 'Green nanotechnologies: synthesis of metal nanoparticles using plants', *Acta Naturae*, 2014, **6**, (1), pp. 35–44

[20] Gowramma, B., Keerthi, U., Mokula, R., et al.: 'Biogenic silver nanoparticles production and characterization from native strain of corynebacterium species and its antimicrobial activity', *3 Biotech*, 2015, **5**, (2), pp. 195–201

[21] Khadar, A., Behara, D.K., Kumar, M.K.: 'Synthesis and characterization of controlled size TiO<sub>2</sub> nanoparticles via green route using *Aloe vera* extract', *Int. J. Sci. Res.*, 2016, **5**, (11), pp. 1913–1916

[22] Sundarajan, M., Gowri, S.: 'Green synthesis of titanium dioxide nanoparticles by *Nyctanthes arbor-tristis* leaves extracts', *Chalcogenide Lett.*, 2011, **8**, (8), pp. 447–451

[23] Abdul Jalil, R.D.H., Nuaman, R.S., Abd, A.N.: 'Biological synthesis of titanium dioxide nanoparticles by *Curcuma longa* plant extract and study its biological properties', *World Sci. News*, 2016, **49**, (2), pp. 204–222

[24] Seabra, A.B., Duran, N.: 'Nitric oxide-releasing vehicles for biomedical applications', *J. Mater. Chem.*, 2010, **20**, pp. 1624–1637

[25] Goh, P.S., Ng, B.C., Lau, W.J., et al.: 'Inorganic nanomaterials in polymeric ultrafiltration membranes for water treatment', *Purification Rev.*, 2015, **44**, pp. 216–249

[26] Allahverdiyev, A.M., Abamor, E.S., Bagirova, M., et al.: 'Antimicrobial effects of TiO<sub>2</sub> and Ag<sub>2</sub>O nanoparticles against drug-resistant bacteria and *Leishmania* parasites', *Future Microbiol.*, 2011, **6**, (8), pp. 933–940

[27] Chen, X., Mao, S.S.: 'Titanium dioxide nanomaterials: synthesis, properties, modifications, and applications', *Chem. Rev.*, 2007, **107**, pp. 2891–2959

[28] Abdul Jalil, R.D.H., Yousef, A.M.: 'Comparison the phytotoxicity of TiO<sub>2</sub> nanoparticles with bulk particles on amber 33 variety of rice (*Oryza sativa*) in vitro', *Sch. Acad. J. Biosci.*, 2015, **3**, (3), pp. 254–262

[29] Hu, C., Lan, Y., Qu, J., et al.: 'Ag/AgBr/TiO<sub>2</sub> visible light photocatalyst for destruction of azodyes and bacteria', *J. Phys. Chem. B*, 2006, **110**, pp. 4066–4072

[30] Abass, R.H., Haleem, A.M., Hamid, M.K., et al.: 'Antimicrobial activity of TiO<sub>2</sub> NPs against *Escherichia coli* ATCC 25922 and *Staphylococcus aureus* ATCC 25923', *Int. J. Comput. Appl. Sci.*, 2017, **2**, (1), pp. 6–10

[31] Stankic, S., Suman, S.S., Haque, F., et al.: 'Pure and multi metal oxide nanoparticles: synthesis, antibacterial and cytotoxic properties', *J. Nanobiotechnol.*, 2016, **14**, p. 73: 1–20

[32] Perez-Espitia, P.J., Ferreira-Soares, N.F., dos Reis Coimbra, J.S., et al.: 'Zinc oxide nanoparticles: synthesis, antimicrobial activity and food packaging applications', *Food Bioprocess Technol.*, 2012, **5**, pp. 1447–1464

[33] Duran, N., Seabra, A.B.: 'Metallic oxide nanoparticles: state of the art in biogenic syntheses and their mechanisms', *Appl. Microbiol. Biotechnol.*, 2012, **95**, (2), pp. 275–288

[34] Muranyi, P., Schraml, C., Wunderlich, J.: 'Antimicrobial efficiency of titanium dioxide-coated surfaces', *J. Appl. Microbiol.*, 2010, **108**, (6), pp. 1966–1973

[35] Abdul Jalil, R.D.H., Ali, A.M.: 'Stimulate the antimicrobial activity of TiO<sub>2</sub> nanoparticles (NPs) using methanol extract of *Citrullus colocynthis*', *Sch. Acad. J. Pharm.*, 2016, **5**, (8), pp. 326–332

[36] Naveen, H.K.S., Kumar, G., Karthik, L., et al.: 'Extracellular biosynthesis of silver nanoparticles using the filamentous fungus *Penicillium* sp.', *Arch. Appl. Sci. Res.*, 2010, **2**, (6), pp. 161–167

[37] Ba-Abbad, M.M., Kadhum, A.H., Mohamad, A.B., et al.: 'Synthesis and catalytic activity of TiO<sub>2</sub> nanoparticles for photochemical oxidation of concentrated chlorophenols under direct solar radiation', *Int. J. Electrochem. Sci.*, 2012, **7**, pp. 4871–4888

[38] Meshram, R.S., Suryavanshi, B.M., Thombre, R.M.: 'Structural and optical properties of CdS thin films obtained by spray pyrolysis', *Adv. Appl. Sci. Res.*, 2012, **3**, p. 1563

[39] Cullity, B.D.: 'Elements of X-ray diffraction' (Addison Wesley, London, 1978, 2nd edn.), p. 531

[40] Wei, W., Mao, X., Ortiz, L.A., et al.: 'Oriented silver oxide nanostructures synthesized through a template-free electrochemical route', *J. Mater. Chem.*, 2011, **21**, (2), pp. 432–438

[41] Jobst, P.J., Stenzel, O., Schürmann, M., et al.: 'Optical properties of unprotected and protected sputtered silver films: surface morphology vs. UV/VIS reflectance', *Adv. Opt. Technol.*, 2013, **3**, pp. 91–102

[42] National Committee for Clinical Laboratory Standards: 'Methods for dilution antimicrobial susceptibility tests for bacteria that grow aerobically: approved standard M7-A' (NCCLS, Villanova, PA, 1986)

[43] Bijnisdorp, I.V., Giovannetti, E., Peters, G.J.: 'Analysis of drug interactions', *Methods Mol. Biol.*, 2011, **731**, pp. 421–434

[44] Vijayalakshmi, R., Rajendran, V.: 'Synthesis and characterization of nano-TiO<sub>2</sub> via different methods', *Arch. Appl. Sci. Res.*, 2012, **4**, (2), pp. 1183–1190

[45] Reddy, K.M., Manorama, S.V., Reddy, A.R.: 'Bandgap studies on anatase titanium dioxide nanoparticles', *Mater. Chem. Phys.*, 2002, **78**, pp. 239–245

[46] Yin, W., Chen, S., Yang, J., et al.: 'Effective band gap narrowing of anatase TiO<sub>2</sub> by strain along a soft crystal direction', *Appl. Phys. Lett.*, 2010, **96**, (22), pp. 221901–221903

[47] Ganesan, S., Babu, I.G., Mahendran, D., et al.: 'Green engineering of titanium dioxide nanoparticles using *Ageratina altissima* (L.)', King & H.E. Robines. medicinal plant aqueous leaf extracts for enhanced photocatalytic activity', *Ann. Phytomed.*, 2016, **5**, (2), pp. 69–75

[48] Bystrická, J., Musilová, J., Vollmannová, A., et al.: 'Bioactive components of onion (*Allium cepa* L.). A review', *Acta Alimentaria*, 2013, **42**, (1), pp. 11–22

[49] Arnault, I., Auger, J.: 'Seleno-compounds in garlic and onion', *J. Chromatogr. A*, 2006, **1112**, (1–2), pp. 23–30

[50] Hubbard, G.P., Wolfram, S., de-Vos, R., et al.: 'Ingestion of onion soup high in quercetin inhibits platelet aggregation and essential components of the collagen-stimulated platelet activation pathway in man: a pilot study', *Br. J. Nutr.*, 2006, **96**, (3), pp. 482–488

[51] Lanzotti, V.: 'The analysis of onion and garlic', *J. Chromatogr.*, 2006, **1112**, (1–2), pp. 3–22

[52] Parida, U.K., Bindhani, B.K., Nayak, P.: 'Green synthesis and characterization of gold nanoparticles using onion (*Allium cepa*) extract', *World J. Nano Sci. Eng.*, 2011, **1**, (4), pp. 93–98

[53] Abdul Jalil, R.D.H., Jawad, M.M.H.M., Abd, A.N.: 'Plants extracts as green synthesis of zirconium oxide nanoparticles', *J. Genet. Environ. Res. Conserv.*, 2017, **5**, (1), pp. 6–23

[54] Shipra Deep Karmakar, S., Khare, R.S., et al.: 'Development of probiotic candidate in combination with essential oils from medicinal plant and their

- effect on enteric pathogens: a review', *Gastroenterol. Res. Pract.*, 2012, (6), pp. 1–6
- [55] Al-Ani, I., Zimmermann, S., Reichling, J., *et al.*: 'Pharmacological synergism of bee venom and melittin with antibiotics and plant secondary metabolites against multi-drug resistant microbial pathogens', *Phytomedicine*, 2015, **22**, (2), pp. 245–255
- [56] Mandal, S., Debmandal, M., Pal, N.K., *et al.*: 'Synergistic anti-*Staphylococcus aureus* activity of amoxicillin in combination with *Emblia officinalis* and *Nymphae odorata* extracts', *Asian Pac. J. Tropical Med.*, 2010, **3**, (9), pp. 711–714
- [57] Rakholiya, K., Chanda, S.: 'In vitro interaction of certain antimicrobial agents in combination with plant extracts against some pathogenic bacterial strains', *Asian Pac. J. Tropical Biomed.*, 2012, **2**, (2), pp. S1466–S1470
- [58] Padalia, H., Moteriya, P., Baravalia, Y., *et al.*: 'Antimicrobial and synergistic effects of some essential oils to fight against microbial pathogens – a review', in Méndez-Vilas, A. (Ed.): 'The battle against microbial pathogens: basic science, technological advances and educational programs' (Formatex Research Center, Zurbaran, Badajoz, Spain, 2015), pp. 34–45
- [59] Grande, M.J., López, R.L., Abriouel, H., *et al.*: 'Treatment of vegetable sauces with enterocin AS-48 alone or in combination with phenolic compounds to inhibit proliferation of *Staphylococcus aureus*', *J. Food Prot.*, 2007, **70**, (2), pp. 405–411
- [60] Sharma, N., Jandaik, S., Kumar, S.: 'Synergistic activity of doped zinc oxide nanoparticles with antibiotics: ciprofloxacin, ampicillin, fluconazole and amphotericin B against pathogenic microorganisms', *Ann. Br. Acad. Sci.*, 2016, **88**, (3), pp. 1689–1698